Hybrid Analytical Model for AC Copper Loss Computation of Hairpin Winding

Du, Yunlu; Huang, Yunkai; Guo, Baocheng; Peng, Fei; Yao, Yu; Dong, Jianning

DOI
10.1109/TMAG.2023.3300305

Publication date
2023

Document Version
Final published version

Published in
IEEE Transactions on Magnetics

Citation (APA)
Du, Y., Huang, Y., Guo, B., Peng, F., Yao, Y., & Dong, J. (2023). Hybrid Analytical Model for AC Copper Loss Computation of Hairpin Winding. *IEEE Transactions on Magnetics*, *60*(3), 1-4. Article 6300104. https://doi.org/10.1109/TMAG.2023.3300305

Hybrid Analytical Model for AC Copper Loss Computation of Hairpin Winding

Yunlu Du [1], Yunkai Huang [1], Baocheng Guo [2], Fei Peng [1], Yu Yao [1], and Jianning Dong [3]

[1]School of Electrical Engineering, Southeast University, Nanjing 210096, China
[2]School of Electrical and Automation Engineering, Nanjing Normal University, Nanjing 210023, China
[3]Department of Electrical Sustainable Energy, Delft University of Technology, 2628 CD Delft, The Netherlands

This article proposes a hybrid analytical model (HAM) for predicting ac copper losses in hairpin windings. The HAM combines the nonlinear semi-analytical model (SAM) and the 1-D ac copper loss computation model to solve the inaccurate boundary solutions of the 1-D ac copper loss computation model when magnetic saturation occurs in the stator teeth. The HAM is used to study the ac losses of the hairpin windings with four different conductor arrangements under different current excitation conditions, and the versatility of the HAM is verified. The HAM has high calculation accuracy, and the calculation speed is 66% faster than the finite element (FE) model. The primary contribution of this research is to present a quick and simple approach for accurately predicting ac copper losses in hairpin windings with arbitrary conductor arrangements.

***Index Terms*—AC copper loss, hairpin winding, hybrid analytical model (HAM), magnetic saturation.**

I. INTRODUCTION

HAIRPIN winding has been extensively utilized in electric vehicle traction motors due to its advantages of high slot filling factor, good heat dissipation performance, and short-end winding [1]. Compared with round copper wire, although the use of hairpin windings can improve torque density, improve efficiency, reduce vibration, noise, etc., at high frequencies, due to the larger cross-sectional area of hairpin windings, the skin effect and proximity effect are exacerbated, resulting in an increase in ac copper loss [2]. Therefore, accurately predicting ac copper loss with different conductor arrangements is essential for reducing ac copper loss.

Although the finite element (FE) model can accurately predict the magnetic field distribution (MFD) and the ac copper loss of the hairpin windings, the computation speed will be significantly slower while eddy current loss conditions are taken into account [3]. To solve the aforementioned problems, scholars have proposed the 1-D ac loss model [4], the 2-D ac loss model [5], and the hybrid calculation model [6]. The 1-D loss model already has an acceptable degree of precision because the magnetic fields in the hairpin winding motor slots are approximately parallel (assuming only the tangential component). However, as the saturation of the stator teeth deepens, there will be inaccuracies in the boundary condition solutions. Therefore, the traditional 1-D model is no longer applicable. To solve the problem of inaccurate boundary conditions when the stator teeth are saturated, a hybrid analytical model (HAM) is proposed in this article. Additionally, the HAM proposed in this article does not need the assistance of expensive FE software, in contrast to current hybrid computational model [6]. The HAM combines the nonlinear semi-analytical model (SAM) [7], [8], [9] and 1-D ac copper loss computation model, which can solve the ac copper loss under different excitation conditions.

The main contribution of this article is to propose a HAM for fast and accurate calculation of ac copper loss of hairpin windings, which is suitable for any conductor configuration.

II. HYBRID ANALYTICAL MODEL

The studied motor has eight-layer hairpin windings, and the effects of the four conductor arrangements [as shown in Fig. 1(a)–(d)] on the ac loss are studied respectively. Fig. 1(e) shows the 1-D ac loss calculation model in the slot.

The derivation of the 1-D ac loss computation model is elaborated in [4] and [10], and hence, is not repeated here. Then, according to the computation model in Fig. 1(e), the ac loss of each conductor can be obtained by the following equation:

$$P = \frac{L_{\mathrm{ef}} b_s \alpha}{\sigma'[\cosh(2\alpha h) - \cos(2\alpha h)]} \cdot \left\{ \begin{array}{c} \left(H_t^2 + H_b^2\right)[\sinh(2\alpha h) + \sin(2\alpha h)] \\ -4 H_t H_b \cos(\varphi_t - \varphi_b) \\ \cdot [\cos(\alpha h)\sinh(\alpha h) + \sin(\alpha h)\cosh(\alpha h)] \end{array} \right\} \tag{1}$$

where L_{ef} is the effective length of the conductor; H_b and H_t are the moduli of the magnetic intensity vectors $\boldsymbol{H_b}$ and $\boldsymbol{H_t}$ on the upper and lower boundaries of the conductor, respectively; φ_b and φ_t are the phases of $\boldsymbol{H_b}$ and $\boldsymbol{H_t}$, respectively; σ' is the equivalent conductivity of conductor.
where

$$\sigma' = \frac{b_w}{b_s}\sigma \tag{2}$$

$$\alpha = 1/\delta = \sqrt{\mu\sigma'\omega/2} \tag{3}$$

where σ is the actual conductivity and δ is the skin depth.

Manuscript received 8 June 2023; revised 11 July 2023; accepted 27 July 2023. Date of publication 1 August 2023; date of current version 27 February 2024. Corresponding author: Y. Huang (e-mail: huangyk@seu.edu.cn).

Color versions of one or more figures in this article are available at https://doi.org/10.1109/TMAG.2023.3300305.

Digital Object Identifier 10.1109/TMAG.2023.3300305

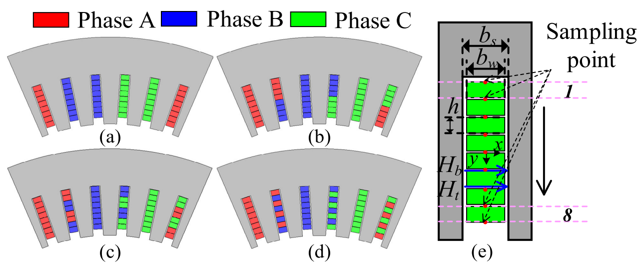

Fig. 1. Illustration of different conductor arrangements in hairpin windings. (a) Conductor arrangement a. (b) Conductor arrangement b. (c) Conductor arrangement c. (d) Conductor arrangement d. (e) Illustration of 1-D ac loss computation model.

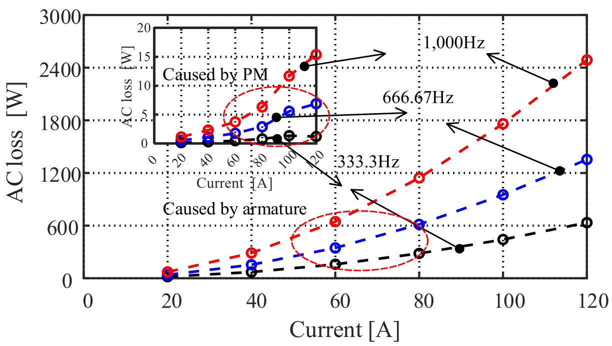

Fig. 2. Separation of ac losses caused by PM and armature.

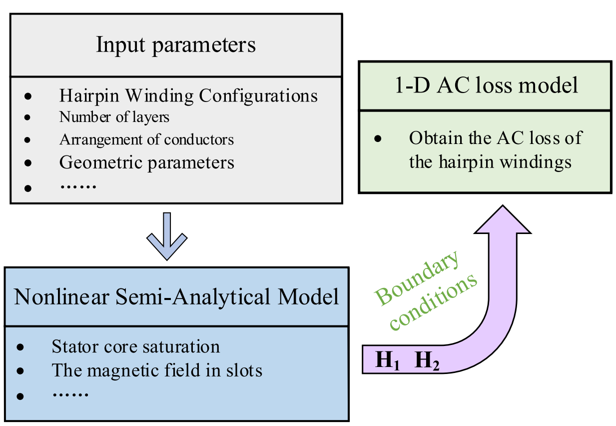

Fig. 3. Flowchart of HAM.

It can be found from (1) that the ac loss can be calculated as long as the boundary magnetic intensity vectors $\boldsymbol{H_b}$ and $\boldsymbol{H_t}$ of each conductor are obtained.

The ac loss caused by the permanent magnet (PM) and the armature is separated according to the frozen permeability method, as shown in Fig. 2. It can be seen that the ac loss caused by the PM is very small.

Then, the nonlinear SAM introduced in [7], [8], and [9] is used to accurately obtain the magnetic intensity vectors of each conductor boundary. All electromagnetic parameters in this model are expressed in terms of complex Fourier series. By introducing a magnetic vector potential A, the magnetic field in slots/teeth can be computed by solving the following Poisson's matrix equations:

$$\frac{\partial^2 \boldsymbol{A}_z^k\big|_r}{\partial r^2} + \frac{1}{r}\frac{\partial \boldsymbol{A}_z^k\big|_r}{\partial r} - \left(\frac{\boldsymbol{V}^k}{r}\right)^2 \boldsymbol{A}_z^k\big|_r = -\boldsymbol{\mu}_{c,\theta}^k \boldsymbol{J}_z - \frac{\mu_0}{r}\left(\boldsymbol{M}_\theta^k + j\boldsymbol{K}_\theta \boldsymbol{M}_r^k\right) \quad (4)$$

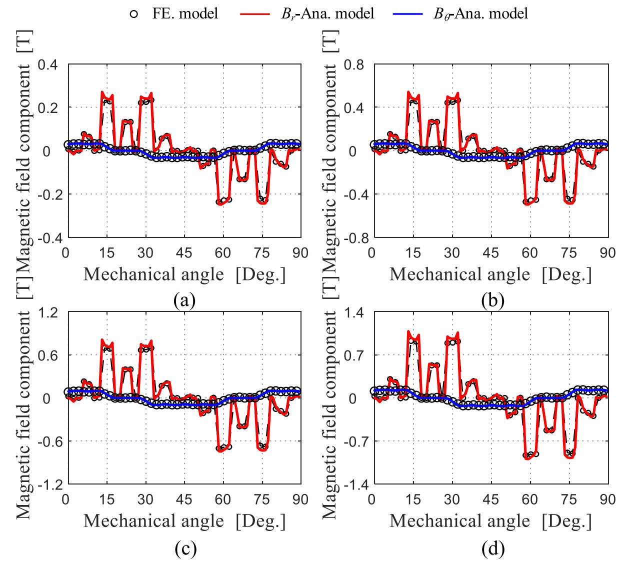

Fig. 4. Comparison of magnetic flux density components in the center of stator slots/teeth (conductor arrangement a). (a) $I_{\text{peak}} = 30$ A. (b) $I_{\text{peak}} = 60$ A. (c) $I_{\text{peak}} = 90$ A. (d) $I_{\text{peak}} = 120$ A.

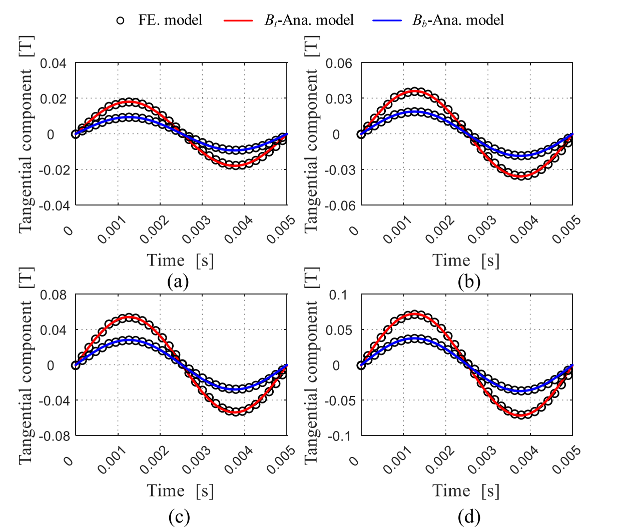

Fig. 5. Tangential component of the magnetic flux density at a sampling point during an electrical period (conductor arrangement a). (a) $I_{\text{peak}} = 30$ A. (b) $I_{\text{peak}} = 60$ A. (c) $I_{\text{peak}} = 90$ A. (d) $I_{\text{peak}} = 120$ A.

$$\boldsymbol{V} = \boldsymbol{\mu}_{c,\theta}\boldsymbol{K}_\theta\left[\boldsymbol{\mu}_{c,r}\right]^{-1}\boldsymbol{K}_\theta \quad (5)$$

$$\boldsymbol{K}_\theta = \text{diag}[-N,\ldots,N] \quad (6)$$

where N is the maximum spatial harmonic order.

Then, the radial and tangential components of the magnetic intensity vector $\boldsymbol{H}$ can be obtained

$$\boldsymbol{H}_r = -j\frac{1}{r}\boldsymbol{\mu}_{c,r}^{-1}\boldsymbol{K}_\theta \boldsymbol{A}_z \quad (7)$$

$$\boldsymbol{H}_\theta = -\boldsymbol{\mu}_{c,\theta}^{-1}\frac{\partial \boldsymbol{A}_z}{\partial r}. \quad (8)$$

Finally, a general ac loss calculation model is proposed by combining SAM and 1-D ac loss computation model. The flowchart is shown in Fig. 3. In this article, the nonlinear iterative algorithm introduced in [8] and [9] is used to consider the nonlinear magnetic saturation of the ferromagnetic material, and hence, is not repeated here.

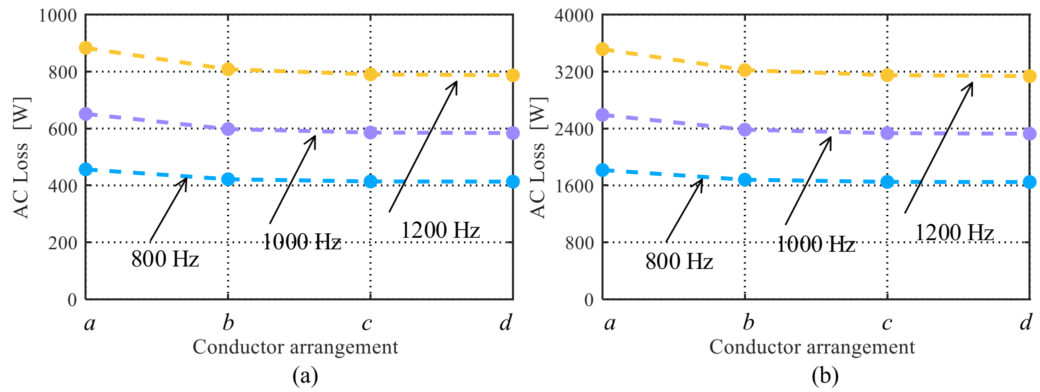

Fig. 6. AC loss calculated by the HAM under different conductor arrangements. (a) $I_{\text{peak}} = 60$ A. (b) $I_{\text{peak}} = 120$ A.

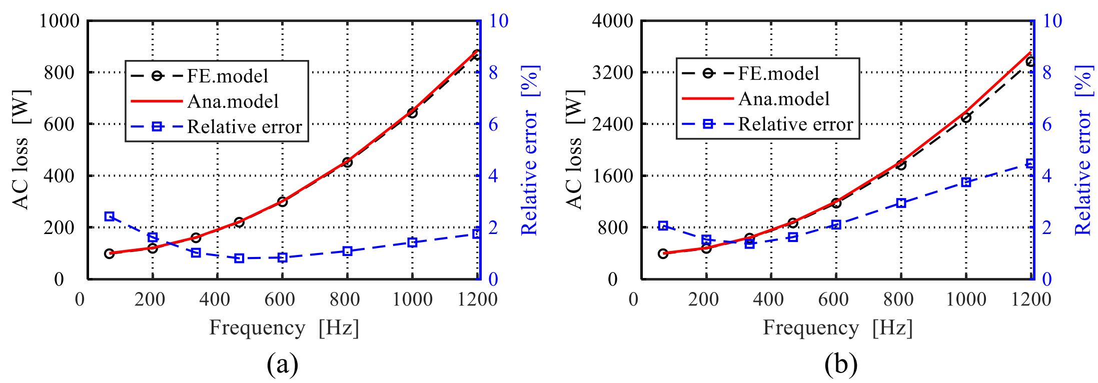

Fig. 7. Comparison of ac loss calculated by HAM and FE model of conductor arrangement a. (a) $I_{\text{peak}} = 60$ A. (b) $I_{\text{peak}} = 120$.

III. FE Model Verification

A. Comparison of Magnetic Flux Density

The effectiveness of the proposed HAM is verified by the FE model. Fig. 4 shows the MFD of the stator slots/teeth center. It can be seen that the analytical model is in good agreement with the FE model. In particular, Fig. 5 shows the variation of the tangential magnetic field component of a conductor boundary in an electrical period under different current excitations. It can be seen that the nonlinear SAM can accurately predict the MFD. That is, the boundary magnetic intensity vectors $\boldsymbol{H_b}$ and $\boldsymbol{H_t}$ of each conductor can be accurately obtained.

B. Comparison of AC Losses

Fig. 6 shows the ac losses calculated by the HAM with different conductor arrangements [i.e., Fig. 1(a)–(d)] under different current excitation (i.e., $I_{\text{peak}} = 60$ and 120 A). It can be seen that with the increase of frequency, the proximity effect and skin effect of the conductor are aggravated, and the ac copper loss of the hairpin winding is increased. In particular, taking conductor arrangement a [i.e., Fig. 1(a)] as an example (when $I_{\text{peak}} = 120$ A), when the frequency increases from 800 to 1200 Hz, the ac copper loss increases from 1.8 to 3.5 kW. In addition, under the same current excitation, the ac loss of conductor arrangement a [i.e., Fig. 1(a)] is the largest. As the number of interleaving conductors of different phases increases [i.e., Fig. 1(b)–(d)], the ac loss of the hairpin winding decreases, and conductor arrangement d [i.e., Fig. 1(d)] is the smallest.

To illustrate the calculation accuracy of the HAM proposed in this article, Fig. 7 shows the comparison between the HAM and the FE model of the ac copper loss of conductor arrangement a [i.e., Fig. 1(a)] under different current excitations. When $I_{\text{peak}} = 120$ A, the minimum relative error between the HAM and the FE model is 1.36% (i.e., when frequency = 333.33 Hz, the ac copper loss calculated by the HAM and the FE model is 641.95 and 633.33 W, respectively), while the maximum relative error is only 4.47% (i.e., when frequency = 1200 Hz, the ac copper loss calculated by the HAM and the FE model is 3515.82 and 3365.24 W, respectively), which meets the engineering calculation accuracy.

C. Comparison of Calculation Time

According to the above analysis, the calculation results of the HAM proposed in the article are in good agreement with the FE model. The FE model with eddy current calculation, on the other hand, requires smaller mesh generation of the conductor to account for the skin effect and proximity effect, resulting in a larger number of meshes and a longer computation time. However, the HAM is based on the analytical solution of the electromagnetic field, which reduces calculation time while maintaining calculation accuracy. For the HAM, the maximum spatial harmonic order is set to $N = 200$; for the FE model, the number of elements is 38 474. The computation time of different methods for ac losses is shown in Table I. It can be observed that compared to the FE model, HAM is 66% faster.

TABLE I
COMPARISON OF CALCULATION TIME

	HAM/s	FE model
Computation time	6min25s	18min51s

TABLE II
INDUCTANCE AND DC RESISTANCE OF THE PROTOTYPE

	Inductance	DC R
Value	104.4 μH	9.74 mΩ

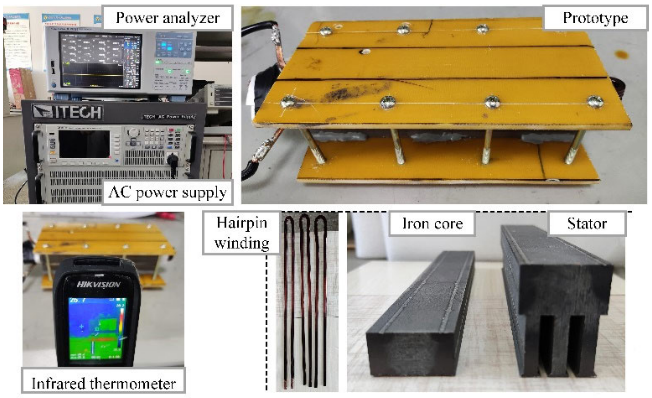

Fig. 8. AC loss measurement experiment.

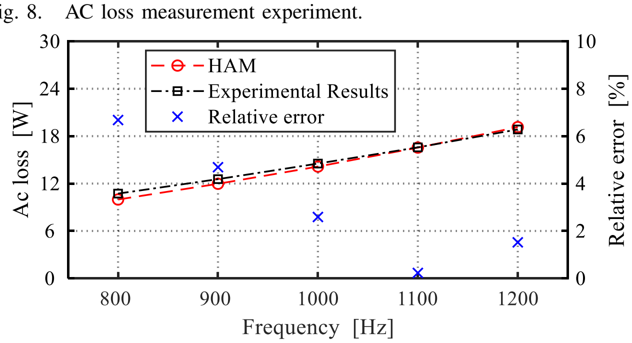

Fig. 9. Comparison of the HAM with the experimental results under ac current input ($I_{rms} = 20$ A).

IV. EXPERIMENTAL VALIDATION

To verify the accuracy of the HAM, a loss test prototype was manufactured, which consists of a partial stator core, hairpin windings, and an iron core. The prototype has eight layers of conductors, and the size of the conductor is 2 × 4 mm. The inductance and dc resistance of the prototype are shown in Table II.

The ac losses experimental platform is shown in Fig. 8. The ac power supply inputs ac current of different frequencies to the prototype, and the power analyzer measures the voltage, current, and loss of the prototype. In addition, to consider the effect of temperature on the resistivity of conductors, the infrared thermometer is used to monitor the temperature of the prototype.

The ac power supply inputs an ac current with an rms value of 20 A to the prototype (frequency range: 800–1200 Hz), and the total loss of the prototype at different frequencies is measured. The measured ac copper loss of the effective part of the conductor in the slot is compared with the results of the HAM proposed in this article, as shown in Fig. 9. It can be seen that with the increase of frequency, the skin effect and proximity effect are aggravated, and the ac copper loss increases significantly. Under the same current excitation, the ac copper loss at 1200 Hz is twice as much as that at 800 Hz. When the frequency is 1200 Hz, the ac copper loss measured by the experiment is 18.85 W, and the ac copper loss calculated by the HAM is 19.14 W, and the relative error is only 1.52%. This shows that the HAM proposed in this article has high calculation accuracy.

V. CONCLUSION

In this article, a new HAM for ac copper loss computation of hairpin windings is proposed, which solves the problem of inaccurate boundary condition calculation when ferromagnetic material is saturated. Meanwhile, compared with the FE model, the computation time is reduced by two-thirds, while the maximum relative error of HAM is still less than 5%. The ac losses at different frequencies are measured for one of the conductor arrangements, the results of the HAM are in good agreement with the experimental results. In addition, through the analysis of the above four conductor arrangements, it can be found that the ac loss of the hairpin winding decreases with the increase of the number of interleaving conductors of different phases. This also shows that the HAM proposed in this article is suitable for hairpin windings with arbitrary conductor arrangement.

ACKNOWLEDGMENT

This work was supported in part by the National Natural Science Foundation of China under Grant 52277036.

REFERENCES

[1] Y. Zhao, D. Li, T. Pei, and R. Qu, "Overview of the rectangular wire windings AC electrical machine," *CES Trans. Electr. Mach. Syst.*, vol. 3, no. 2, pp. 160–169, Jun. 2019, doi: 10.30941/CESTEMS.2019.00022.

[2] E. Preci et al., "Hairpin windings: Sensitivity analysis and guidelines to reduce AC losses," in *Proc. IEEE Workshop Elect. Mach. Design, Control Diagnosis (WEMDCD)*, Apr. 2021, pp. 82–87, doi: 10.1109/WEMDCD51469.2021.9425643.

[3] M. Aoyama and J. Deng, "Visualization and quantitative evaluation of eddy current loss in bar-wound type permanent magnet synchronous motor for mild-hybrid vehicles," *CES Trans. Electr. Mach. Syst.*, vol. 3, no. 3, pp. 269–278, Sep. 2019, doi: 10.30941/CESTEMS.2019.00035.

[4] L. Chen, W. Cai, T. Chen, and F. Chai, "AC copper loss analytic modle considering for multiple hairpin winding configurations," in *Proc. IEEE 5th Int. Electr. Energy Conf. (CIEEC)*, May 2022, pp. 3984–3989, doi: 10.1109/CIEEC54735.2022.9845958.

[5] X. Wang, L. Wang, L. Mao, L. Yi, and S. Yang, "Calculation method of winding loss in high frequency planar transformer," in *Proc. Int. Conf. Electr. Syst. Aircr., Railway, Ship Propuls. Road Vehicles Int. Transp. Electrific. Conf. (ESARS-ITEC)*, 2016, pp. 1–5, doi: 10.1109/ESARS-ITEC.2016.7841349.

[6] D. P. Morisco, I. L. Iepure, and A. Moeckel, "Application of a hybrid modeling approach for eddy current estimation in hairpin windings," in *Proc. IEEE Int. Electr. Mach. Drives Conf. (IEMDC)*, May 2019, pp. 2251–2258, doi: 10.1109/IEMDC.2019.8785084.

[7] R. L. J. Sprangers, J. J. H. Paulides, B. L. J. Gysen, and E. A. Lomonova, "Magnetic saturation in semi-analytical harmonic modeling for electric machine analysis," *IEEE Trans. Magn.*, vol. 52, no. 2, pp. 1–10, Feb. 2016, doi: 10.1109/TMAG.2015.2480708.

[8] Z. Djelloul-Khedda, K. Boughrara, F. Dubas, and R. Ibtiouen, "Nonlinear analytical prediction of magnetic field and electromagnetic performances in switched reluctance machines," *IEEE Trans. Magn.*, vol. 53, no. 7, pp. 1–11, Jul. 2017, doi: 10.1109/TMAG.2017.2679686.

[9] H. Zhao, C. Liu, Z. Song, and J. Yu, "A fast optimization scheme of coaxial magnetic gears based on exact analytical model considering magnetic saturation," *IEEE Trans. Ind. Appl.*, vol. 57, no. 1, pp. 437–447, Jan. 2021, doi: 10.1109/TIA.2020.3040142.

[10] D. B. Pinhal and D. Gerling, "A review of the analytical calculation of the AC-resistance of armature windings," in *Proc. 23rd Int. Conf. Electr. Mach. Syst. (ICEMS)*, 2020, pp. 906–911, doi: 10.23919/ICEMS50442.2020.9290963.